Biochimica et Biophysica Acta 903 (1987) 186–196
Elsevier

BBA 73690

Gel-state metastability and nature of the azeotropic points in mixtures of saturated phosphatidylcholines and fatty acids

Rumiana D. Koynova, Athanas I. Boyanov and Boris G. Tenchov

Central Laboratory of Biophysics, Bulgarian Academy of Sciences, Sofia 1113 (Bulgaria)

(Received 6 March 1987)

Key words: Phosphatidylcholine; Fatty acid; Phase diagram; Azeotropic point; Metastability; Differential scanning calorimetry

The temperature-composition phase diagrams of dipalmitoylphosphatidylcholine (DPPC)/palmitic acid and distearoylphosphatidylcholine (DSPC)/stearic acid mixtures in excess water were recorded using high-sensitivity differential scanning calorimetry. New, slowly reversible phase transitions were found at 38°C in DPPC/palmitic acid mixtures at 0.4–0.9 mole fractions of palmitic acid and at 46°C in the DSCP/stearic acid binary. These transitions reveal gel-state metastability of the mixtures which is caused most probably by co-crystallization of the two lipids as it cannot be observed in the pure components. Both mixtures display azeotropic behavior at 2 fatty acids per 1 phospholipid. The physical reasons for such behavior have been analyzed theoretically in the framework of the Bragg-Williams and the UNIversal QUAsiChemical (UNIQUAC) approximations. This analysis shows that the azeotropic points in the phase diagrams are due to a combination of compound formation in the solid state and close to random mixing in the liquid state of the mixtures. UNIQUAC provides better fits to the experimental phase diagrams since it accounts also for the dimer-monomer character of the phospholipid/fatty acid mixtures. At fatty acid mole fractions greater than 0.65–0.7 the excess fatty acids phase separate from the compound phase. The stability of the compound phase domains at low fatty acid concentrations in relation to their possible physiological role has been discussed.

Introduction

The interest in the interaction of free fatty acids with lipid bilayers arises from the strong influence of these compounds on a variety of physiologically important membrane properties, including permeability, enzyme activity, ability to fuse, etc. [1–4]. Valuable insights into this problem have been provided by studies on model membranes using microcalorimetry [5,6], NMR [7–9], X-ray scattering [9]. Microcalorimetric studies on mixtures of DPPC with palmitic acid have shown that increasing molar contents of the fatty acid raise the temperature of the gel-liquid crystal phase transition until a sharp-melting mixture of 1 DPPC : 2 palmitic acid molar ratio is reached [5,6]. A remarkable feature of this mixture is that it melts at a temperature higher than the transition temperatures of both pure components. In phase diagrams terminology, such behavior is due to the existence of a maximum azeotropic (isoconcentra-

Abbreviations: PC, phosphatidylcholine; DPPC, 1,2-dipalmitoyl-*sn*-glycero-3-phosphorylcholine; DSPC, 1,2-distearoyl-*sn*-glycero-3-phosphorylcholine; DSC, differential scanning calorimetry; DTA, differential thermal analysis; NMR, nuclear magnetic resonance

Correspondence: B.G. Tenchov, Central Laboratory of Biophysics, Bulgarian Academy of Sciences, Acad G, Bonchev Street, Bl 21, 1113 Sofia, Bulgaria.

tion) point in the phase diagram of the lipid mixture, where a solid and a liquid phase of the same composition co-exist. The maximum and minimum azeotropic points represent one of the four types of peculiar points in the binary phase diagrams [10]. The DPPC/palmitic acid mixture appears to be the only thus far known example of a lipid binary with a clearly expressed azeotropic point. The mere existence of a peculiar point of this type is an indication for a strongly non-ideal lateral mixing of the two lipids. It has been assumed by Mabrey and Sturtevant [5] that it reflects formation of complexes of 1 PC : 2 fatty acid stoichiometry. However, it is of certain interest to analyze this question on more general grounds and to find out what principal kinds of lateral lipid ordering would lead to appearance of maximum and minimum azeotropic points in the phase diagrams. Such analysis can be applied not only to PC/fatty acid mixtures but also to other lipid binaries where azeotropic behavior can be suspected. For example, the calorimetric results of Van Dijck et al. [11] indicate a minimum azeotropic point for the dielaidoyl PC/dimyristoyl PC mixture, at variance with the spin-label study of Wu and McConnell [12] where a solid-solid phase separation for this mixture was found.

The phase diagrams of the binary lipid mixtures are an ample source of information about the lateral lipid–lipid interactions and ordering because a theoretical simulation of their shape in the framework of various statistical-mechanical approaches allows to determine the values of some non-ideality parameters which describe the magnitude and sign of the deviation from ideal lateral mixing [13–17]. Our purposes here are to establish azeotropic behavior also for the DSPC/stearic acid mixture, to analyze the phase diagrams of the DPPC/palmitic acid and DSPC/stearic acid mixtures and to find out what kinds of non-ideal mixing in gel and liquid crystalline states must combine as to produce the observed azeotropic points. The shape of these phase diagrams was determined from data recorded by high-sensitivity DSC. The calorimetric data revealed also a gel-state metastability of the mixtures which is particularly characteristic of the PC–fatty acid interactions in the solid state as it cannot be observed in the pure components.

Materials and Methods

Synthetic L-DPPC, L-DSPC, palmitic acid (GC reference) and stearic acid (GC reference) (Fluka) were used without further purification. By thin-layer and gas chromatography (TLC and GC) the purity of the phospholipids was shown to be over 99%.

Chloroform solutions of appropriate lipid amounts were mixed, the chloroform removed by rotary evaporation under nitrogen. The lipid was dried under vacuum for at least 4 h. The mixtures were hydrated overnight in doubly-distilled water (pH ~ 5.0, conductivity ~ 10^{-6} $\Omega^{-1} \cdot cm^{-1}$) at room temperature, then equilibrated for 1 h at about 10 Cdeg above their phase transition temperature, and shaken at this temperature on a vortex mixer five times for 1 min with 2-min intervals. The total lipid concentration in all samples studies was in the range 0.3–0.7 mg/ml. The pH values of the lipid dispersions were the same (within $\pm$ 0.05) as those of pure water. Titration of palmitic acid in DPPC bilayers has shown a pK value of about 10 [6]. Therefore we expect that the fatty acids in our samples are in fully protonated state.

The gel-state metastability of the lipid mixtures was studied by storing them at 4° C prior to DSC measurements. L-DPPC/palmitic acid suspensions with mole fraction of palmitic acid up to 0.2 were stored at 4° C for at least 4 days as to induce the appearance of the subtransition. The samples with higher mole fraction of palmitic acid were stored at 4° C for at least 12 days. L-DSPC/stearic acid suspensions with mole fraction of stearic acid up to 0.2 were stored at 4° C for at least 20 days. The sample with 60 mol% stearic acid was stored at 4° C for 9 days.

The thermograms were recorded with a Privalov differential scanning microcalorimeter (DASM-1M). A heating rate of 0.5 Cdeg · min^{-1} was used. The phase transition characteristics (onset, completion, enthalpy) were determined in a standard way [13].

All samples stored at 4° C were scanned twice, the second scan performed immediately after the first one. The cooling of the sample inside the calorimetric cell between two successive heating runs was passive (it is not controllable in a

DASM-1M calorimeter). The time elapsing between end of first scan and start of second scan was about 1 h for these measurements.

Experimental results

(a) Gel-state metastability of PC/fatty acid mixtures

Sequences of DSC scans through the composition range of the two mixtures studied are shown in Figs. 1 and 2. The samples were scanned twice as described in Materials and Methods. The second scans produced practically identical results about the pretransition and the main melting transition, even at high fatty acid contents where the melting of the mixtures proceeds in a rather complex way. As it should be expected, the 'subtransitions' at low fatty acid contents (5–10 mol%) were observed only during the first heating runs. The new transitions found at 38 °C in the DPPC/palmitic acid mixture and at 46 °C in the DSPC/stearic acid mixture were also observed only during the first scans.

The subtransition in DPPC/palmitic acid mixtures disappears at about 5–6 mol% of palmitic acid as reported earlier [18], while the subtransition in the DSPC/stearic acid mixtures persists to about 10 mol% of stearic acid but, as in the previous case, it also decreases without appreciable change in shape and position. The subtransition in the latter mixtures were induced by longer incubation at 4 °C (20 days) compared to the 4-days incubation of DPPC/palmitic acid mixtures in accordance with the results for pure DPPC and DSPC [19,20].

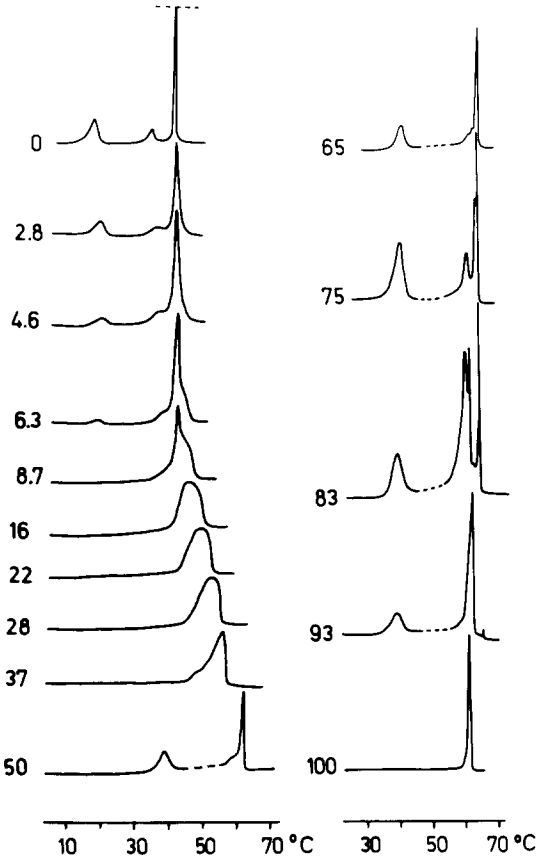

Fig. 1. Sequence of DSC scans of DPPC/palmitic acid mixtures. The transition at 38 °C in the range 50–93 mol% palmitic acid (recorded at 2.5-times greater sensibility) and the subtransition are present only during the first heating scans.

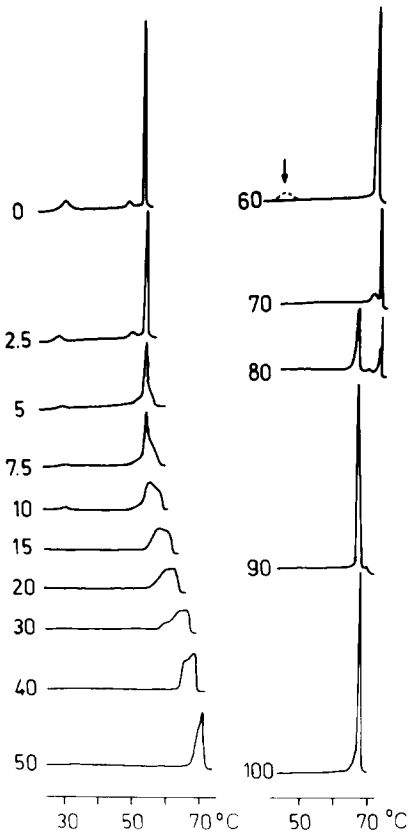

Fig. 2. Sequence of DSC scans of DSPC/stearic acid mixtures. The arrow shows a first-scan transition appearing after 9-days storage of the sample at 4 °C.

A rather prolonged storage of the samples at 4 °C was required to induce the appearance of the phase transition at 46 °C in the DSPC/stearic acid mixtures (Fig. 2, arrow). This transition is very slowly reversible and the example of it shown in Fig. 2 is probably far from its saturated magnitude. We have studied in more detail the properties of the transition at 38 °C in DPPC/palmitic acid mixtures as it has faster kinetics of appearance and saturation (Fig. 3). In the example given in Fig. 3 the transition at 38 °C in a DPPC/palmitic acid mixture saturates for between 3 and 12 days to a final enthalpy of 4.3 kcal/mol. A basic property of this transition is that it appears only in mixtures of appropriate amounts of DPPC and palmitic acid (Figs. 1 and 4). A 40-days storage at 4 °C of samples containing only palmitic acid did not produce even the smallest trace of this transition. On the other hand, it appears only at great enough mole fractions of palmitic acid (more than 0.4) and its maximum enthalpy is reached at about 65–75 mol% of palmitic acid (Figs. 1 and 6). Besides, its $T_m = 38$ °C is about 3.5 °C lower than the temperature of the main transition of pure DPPC. These facts show that this transition can neither be attributed to a phase separation of a more or less pure DPPC phase, nor related to the subtransition, but rather it reflects a low-temperature co-crystallization of DPPC and palmitic acid which requires sufficiently large fractions of both lipids to be present in their mixture. This conclusion will be further discussed in relation with the analysis of the azeotropic points in the phase diagram (Fig. 5).

It is noteworthy that similarly long incubations of the samples at room temperature, which is well below the transition at 38 °C, did not induce its appearance. It seems that, similarly to other crystallization processes, conditions favoring the conversion of the metastable solid state into equilibrium state exist in a restricted temperature interval, and not anywhere below the transition temperature.

In summary, the DSC results identify two unrelated types of gel-state metastability in DPPC/

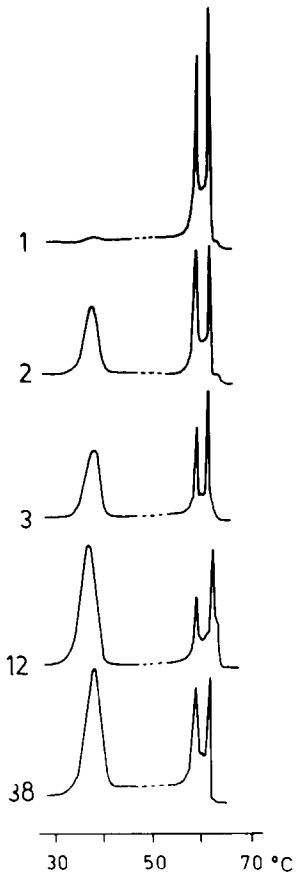

Fig. 3. DSC scans illustrating the kinetics of appearance and saturation of the slowly reversible transition at 38 °C upon sample storage at 4 °C for 1, 2, 3, 12 and 38 days. Sample composition 38 mol% DPPC: 72 mol% palmitic acid. The transition is scaled up 2.5-times compared to the melting transition.

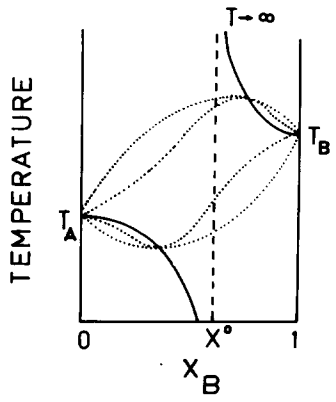

Fig. 4. Schematic presentation of the lines of possible minimum and maximum azeotropic points in a phase diagram (thick lines) and the borderline at X° between them (vertical dashed line) according to Eqns. 5–7.

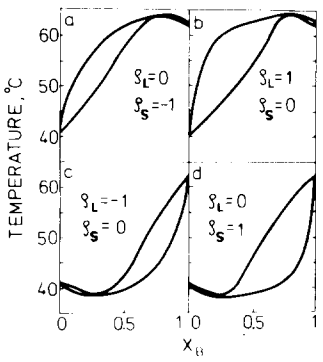

Fig. 5. Model phase diagrams calculated in Bragg-Williams approximation illustrating the conditions for the existence of maximum and minimum azeotropic points.

palmitic acid mixtures. One of them, at low fatty acid content, is due to the subtransition in pure DPPC. The other one, in the range 0.4–0.9 mole fraction of palmitic acid, results most probably from a process of co-crystallization of the two lipids. We believe that the same behavior is characteristic also for DSPC/stearic acid mixtures but on larger time scales.

(b) Shape of PC/fatty acid phase diagrams

The shape of the two PC/fatty acid phase diagrams were determined from DSC data using a previously described procedure [13]. In agreement with the DTA measurements of Schullery et al. [6], the pretransition in DPPC/palmitic acid mixtures shifts upwards and merges into the main transition at less than 10 mol% of palmitic acid (Figs. 1 and 6). The same behavior of the pretransition was observed also in the DSPC/stearic acid mixtures (Figs. 2 and 7).

However, our data about the solidus line of the phase diagrams is clearly at variance with the results of Schullery et al. [6]. While according to Figs. 6 and 7 of the present paper the solid line (onset of the main transition) remains horizontal until disappearance of the pretransition and then it shifts upwards, Schullery et al. [6] have found that the solid line of the DPPC/palmitic acid phase diagram remains horizontal also after disappearance of the pretransition, up to about 25 mol% of palmitic acid. This discrepancy is significant because a horizontal solidus line extended

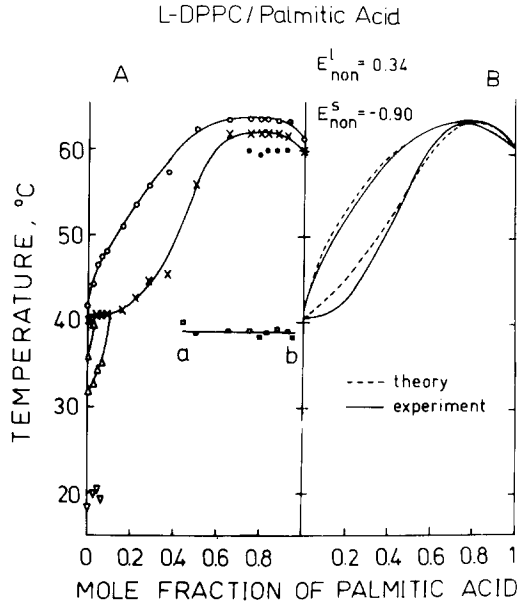

Fig. 6. (A) Experimental phase diagram of the DPPC/palmitic acid mixture. ×, ○, onset and completion of the man transition respectively; △, onset and completion of the pretransition; ▽, midpoint of the subtransition; □, midpoint of the transition at 38 °C; ●, midpoint of the peak corresponding to melting of pure fatty acid. (B) Corrected phase diagram and the best theoretical fit calculated using UNIQUAC. The values of E_{non} are in kT units.

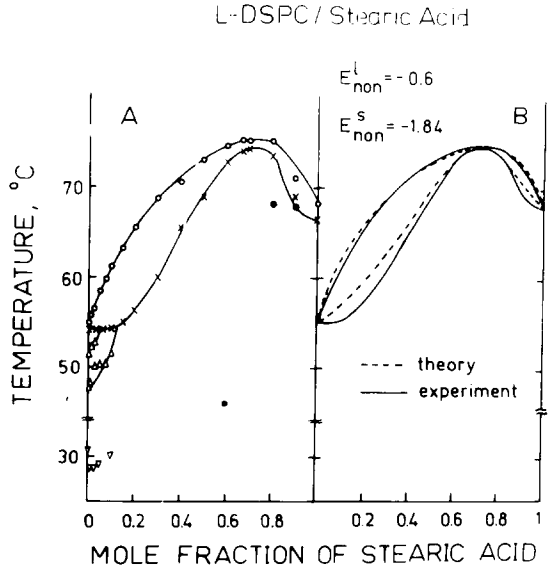

Fig. 7. (A) Experimental phase diagram of the DSPC/stearic acid mixture. Notation as in Fig. 6. (B) Corrected phase diagram and the best theoretical fit calculated using UNIQUAC. The values of E_{non} are in kT units.

beyond the range of the pretransition implies the existence of a quarternary point in the phase diagram which would violate the Gibbs phase rule. To avoid this, Schullery et al. [6] have to assume that the quaternary point is actually split into two triple points (so called 'minor' peritectic points) closely located (within 3 Cdeg) on the temperature scale. Kohn and Schullery [8] presented also NMR evidence supporting this assumption. Our DSC data do not indicate such complex behavior and are consistent with the existence of a single triple point. The reason for this discrepancy is not clear. It may be hidden in the different lipid concentration used; very low concentrations in our DSC study compared to the rather concentrated suspensions used by Schullery et al. [6] and Kohn and Schullery [8] which may require longer equilibration times.

Figs. 1, 2, 6 and 7 show that both PC/fatty acid mixtures studied display clearly expressed azeotropic behavior. The extremely sharp azeotropic peaks (halfwidth of 0.3 Cdeg) appear at about 1 PC:2 fatty acids and are seen in the thermograms up to a 0.8–0.9 mole fraction of fatty acid. The azeotropic point of the DPPC/palmitic acid mixture is at 64°C which is about 3 Cdeg higher than the melting temperature of pure palmitic acid, in agreement with the data of Mabrey and Sturtevant [5] and Schullery et al. [6], while the azeotropic point of the DSPC/stearic acid mixture is at 75°C which is 7 Cdeg higher than the melting temperature of pure stearic acid.

As evident from Figs. 1–3, the melting of the mixtures at mole fractions of fatty acid greater than 0.7 proceeds in a rather complex (but basically reproducible) way. This complexity is not obvious from the thermograms of Schullery et al. [6] which show a single peak in this region. On the other hand, Mabrey and Sturtevant [5] note the complex shape of the transition (although do not illustrate it). However, their pure palmitic acid melts in two peaks located at 57°C and 60°C in disagreement with Schullery et al. [6] (one peak at 62°C) and our data (Fig. 1, 100% palmitic acid). Our experience shows that the double-peak melting of palmitic acid occurs in sonicated samples. In general, our data are roughly consistent with the conclusion for separation of pure palmitic acid in this range (see Discussion).

Analysis of the azeotropic points in PC/fatty acid phase diagrams

The principle of construction of phase diagrams follows directly from the conditions of thermodynamic equilibrium in a multicomponent, multiphase system. These conditions require constant temperature and pressure throughout the system, and equal chemical potentials of the components in the different phases [10]. According to the meaning of a temperature-composition binary phase diagram, the solidus and liquidus lines encircle a region of equilibrium coexistence of the solid and liquid phases. With respect to the conditions stated above, at any fixed temperature, at the intersections with the solidus and liquidus curves the following equations must hold

$$\begin{aligned} \mu_A^{os} + \ln X_A^s + \ln j_A^s &= \mu_A^{ol} + \ln X_A^l + \ln j_A^l \\ \mu_B^{os} + \ln X_B^s + \ln j_B^s &= \mu_B^{ol} + \ln X_B^l + \ln j_B^l \end{aligned} \tag{1}$$

Here A and B denote PC and fatty acid, respectively; s and l denote solid and liquid phase. The standard chemical potentials are related to the enthalpies, ΔH_A and ΔH_B, of the phase transitions of the pure components through the Gibbs-Helmholtz equation

$$\begin{aligned} (\mu_A^{ol} - \mu_A^{os}) \cdot T_A &= \Delta H_A \cdot (T_A - T) \\ (\mu_B^{ol} - \mu_B^{os}) \cdot T_B &= \Delta H_B \cdot (T_B - T) \end{aligned} \tag{2}$$

where T_A and T_B are the melting temperatures of the pure components.

In order to exploit Eqn. 1 for interpretation of the shape of the phase diagrams we need expressions relating the activity coefficients, j_A and j_B, to the parameters of the lateral lipid–lipid interactions and ordering. Because of the lack of exact theory suitable for practical applications, the determination of j is carried out in the framework of various statistical-mechanical approximations. Two basic approximations of this kind are the Bragg-Williams approximation (mean-field theory) and the quasichemical method proposed by Bethe and Peierls for Ising models, and, independently, by Guggenheim. Their physical foundations and underlying assumptions are thoroughly examined in textbooks on statistical physics [21,22]. The former has been frequently used for analysis of phase diagrams of lipid binaries [13,16,23–25]. It is instructive to realize also that a

number of methods developed on seemingly independent grounds [11,15,26,27] turn out to be versions of the Bragg-Williams approximation when applied to binary lipid mixtures. The quasichemical approach has only occasionally been applied for calculations of phase diagrams [14,17,25] although it is thought of as the more advantageous one [21].

In the Bragg-Williams approximation, the activity coefficients can be expressed as [21]

$$\ln f_{A,B} = \rho \cdot (1 - X_{A,B})^2 / kT \tag{3}$$

where $\rho = Z \cdot E_{non}/2$ is an 'energetical' non-ideality parameter, Z is the number of the nearest neighbors in lateral direction, and the non-ideal energy of lateral interactions is

$$E_{non} = 2E_{AB} - E_{AA} - E_{BB} \tag{4}$$

Here E_{AB}, E_{AA} and E_{BB} are the interaction energies of the three different kinds of nearest-neighbor pairs, AB, AA and BB, respectively.

With the aid of Eqns. 1–3 an experimental phase diagram can be simulated by varying the values of ρ_s and ρ_l until the theoretical solidus and liquidus curves fit the experimental ones. The values of ρ_s and ρ_l obtained in this way characterize the lateral lipid mixing in the two phases. The value $\rho = 0$ corresponds to ideal mixing (ideal lens-like phase diagram). $\rho > 0$ reflects clustering of the components which may result in a lateral phase separation for great enough non-ideality, $\rho > \rho_c = kT/2X_A X_B$ [13,17], $\rho < 0$ reflects a 'chessboard' type arrangement of the lipids (formation of compounds).

The major shortcoming of the Bragg-Williams approximation is that a non-ideality correction of the kind shown in Eqn. 3 contributes only to the enthalpy term of the free energy of mixing, while the mixing entropy remains the same as that of an ideal mixture [21]. Nevertheless, we use it here, as, at least qualitatively, it very clearly interprets the reasons for appearance and the physical properties of the azeotropic points. According to their definition, $X_A^s = X_A$ at the azeotropic points. Combining this condition with Eqns. 1–3 it can be easily shown that azeotropic points exist when the following inequalities are satisfied

$$\frac{T_B}{\Delta H_B} \geqslant \frac{T_B - T_A}{\rho_s - \rho_l} \geqslant -\frac{T_A}{\Delta H_A} \tag{5}$$

Maximum azeotropic points appear when $\rho_s - \rho_l < 0$ and minimum points when $\rho_s - \rho_l > 0$, with the simultaneous fulfillment of Eqn. 5. The location, (X_A^{az}, T_{az}), of the azeotropic points on the phase diagram is determined by

$$T_{az} = \frac{T_B}{\Delta H_B}(\rho_s - \rho_l) \cdot (X_A^{az})^2 + T_B \tag{6a}$$

$$X_A^{az} = \frac{T_A \cdot \Delta H_B - \sqrt{D}}{T_A \cdot \Delta H_B - T_B \cdot \Delta H_A} \tag{6b}$$

where

$$D = \Delta H_A \cdot \Delta H_B \cdot T_A \cdot T_B \cdot \left[\frac{T_B - T_A}{\rho_l - \rho_s} \cdot \left(\frac{\Delta H_B}{T_B} - \frac{\Delta H_A}{T_A} \right) + 1 \right]$$

A most important consequence of this analysis is that the azeotropic points cannot be arbitrarily located anywhere out of the range (T_A, T_B) on the phase diagram. They form two different curves (one of them contains only minimum and the other only maximum points) which are shown schematically in Fig. 4. The exact position of these curves in any specific case can be calculated from Eqns. 6a and 6b. The borderline concentration X^o separating these two curves is given by

$$X^o = \frac{T_B \cdot \Delta H_A - \sqrt{\Delta H_A \cdot \Delta H_B \cdot T_A \cdot T_B}}{T_B \cdot \Delta H_A - T_A \cdot \delta H_B} \tag{7}$$

The minimum and maximum points are always located in the ranges $X_B < X^o$ and $X_B > X^o$, respectively, and their temperatures move away from T_A or T_B with X_B getting closer to X^o.

It is pertinent to illustrate the conditions for existence of azeotropic points by several model diagrams calculated in Bragg-Williams approximation (Fig. 5). These calculations show that maximum azeotropic points of the type observed in DPPC/palmitic acid and DSPC/stearic acid mixtures may arise only if $\rho_l - \rho_s > 1\ kT$, or, in terms of non-ideal energy of mixing, $E_{non}^l - E_{non}^s > 0.3$–$0.5\ kT$ depending on the value of Z. The two principally different situations satisfying this condition are shown in Fig. 5a, b. One of them combines ideal mixing in the liquid phase with compound formation in solid state (Fig. 5a, $\rho_l = 0$ and $\rho_s = -1\ kT$), the other combines ideal mixing in solid state with clustering (or phase separation)

of the lipids in liquid state (Fig. 5b, $\rho_s = 0$ and $\rho_l = 1\ kT$). We may accept the former alternative since the latter one seems unlikely for these mixtures, but a more precise formulation would require to say that the azeotropic points in the saturated PC/fatty acid mixtures arise as a consequence of a relatively much stronger attraction between PC and fatty acid molecules in the gel state compared to the liquid crystalline state. As will be shown below, this conclusion remains valid also if the more sophisticated quasichemical approach is applied. It is consistent also with the proposed in the previous section interpretation of the observed gel-state metastability as due to a process of co-crystallization of the two lipids.

A quantitative agreement between the model diagrams in Fig. 5 and the experimental diagrams in Figs. 6 and 7 should not be pursued, at least for the reason that the theoretical method applied is suitable for description of mixtures of lipids of approximately the same size (characterized by the same Z), while the PC/fatty acid mixtures are actually binaries of dimer-monomer type. A cross-section through the hydrophobic region parallel to the lipid-water interface is a two-dimensional triangular lattice formed by the lipid acyl chains. Palmitic acid occupies one site of this lattice, while PC occupies two neighboring sites. It is well known that the configurational entropy of dimer-monomer mixtures strongly differs from that of monomer-monomer mixtures. More suitable for description of mixtures of this type is the UNIversal QUAsiChemical method (UNIQUAC) developed by Abrams and Prausnitz [28] as an extension of the quasichemical approximation encompassing molecular mixtures containing species of different size.

Adapted for two-dimensional dimer-monomer mixtures on a triangular lattice, the general expressions for the activity coefficients derived by Abrams and Prausnitz [28] obtain the form

$$\ln f_A = \ln \frac{\Phi_A}{X_A} + 4 \cdot \ln \frac{\Theta_A}{\Phi_A} + \Phi_B - \tfrac{4}{3} \ln(\Theta_A + \Theta_B \tau) + \frac{4\Theta_B}{3}\left(\frac{\tau}{\Theta_A + \Theta_B \tau} - \frac{\tau}{\Theta_B + \Theta_A \tau}\right) \tag{7a}$$

$$\ln f_B = \ln \frac{\Phi_B}{X_B} + 3 \cdot \ln \frac{\Theta_B}{\Phi_B} - \tfrac{1}{2}\Phi_A - \ln(\Theta_B + \Theta_A \tau) + \Theta_A\left(\frac{\tau}{\Theta_B + \Theta_A \tau} - \frac{\tau}{\Theta_A + \Theta_B \tau}\right) \tag{7b}$$

where

$$\tau = \exp(-E_{non}/2kT);$$

$$\Theta_A = \frac{4X_A}{3X_B + 4X_A};\quad \Theta_B = \frac{3X_B}{3X_B + 4X_A};$$

$$\Phi_A = \frac{2X_A}{X_B + 2X_A};\quad \Phi_B = \frac{X_B}{X_B + 2X_A}$$

The non-ideal energy in Eqns. 7a and 7b is given again by Eqn. 4 but with E_{AB}, E_{AA} and E_{BB} defined as interaction energies between neighboring lattice sites occupied by monomers B and one half of the dimers A.

Using Eqns. 7a and 7b instead of Eqn. 3 in the simulation of the phase diagrams we obtain the show in Figs. 6b and 7b best theoretical fits to the experimental diagrams. The experimental phase diagrams were corrected with respect to the finite width of the phase transitions in the pure components as described by Lee [13]. It can be seen that the maximum azeotropic points observed in the two PC/fatty acid mixtures are due to a difference between 'solid' and 'liquid' non-ideal interaction energies of about 1.2 kT ($E^s_{non} - E^l_{non} \approx -1.2\ kT$ with values of E^l_{non} closer to zero). Therefore, the general qualitative conclusion is the same as that obtained from the Bragg-Williams approximation, these phase diagrams result from a stronger attraction between the two lipids in the solid state than in the liquid state. Quantitatively, the application of UNIQUAC is justified for at least two reasons. First, this method provides better fits to the experimental phase diagrams than the Bragg-Williams approximation. This is a certain indication for the important influence of the dimer-monomer character of the mixtures on the shape of the phase diagrams. Second, the best fits are reached at negative values of E^s_{non} and closer to zero values of E^l_{non}. This allows us to resolve the ambiguity illustrated by Fig. 5a, b and to conclude that the azeotropic behavior of the PC/fatty acid mixtures is due to a combination of compound formation in solid state with close to

ideal mixing in liquid state. It appears also that the tendency to compound formation is stronger in the DSPC/stearic acid mixture compared to the DPPC/palmitic acid mixture.

Discussion

The theoretical analysis of the conditions for azeotropic behavior and the simulation of the experimental phase diagrams provide clear indications for compound formation between PC and fatty acid in the solid state of the mixtures. The fatty acids may act in this case as spacers setting apart the PC molecules and reducing in this way the steric repulsion between the bulky head groups of the PC molecules in the gel state. Also conceivable is a preferential PC-fatty acid hydrogen bonding which might be better consistent with a strict 1:2 stoichiometry of the compounds. The compound gel phase is metastable at low temperatures and converts slowly to an equilibrium crystalline phase (designated as L_c^{com} in Fig. 8) which is stable up to 38°C in DPPC/palmitic acid mixtures and up to 46°C in DSPC/stearic acid mixtures. The DSC evidence provides strong support in favor of lipid co-crystallization in this phase – this type of metastability cannot be observed in the pure components and the maximum enthalpy of the transition at 38°C is reached at 65–75 mol% of palmitic acid where presumably all lipids are incorporated in the compound phase. This conclusion is confirmed also by our preliminary X-ray observations of the L_c^{com} phase (Koynova, R., Laggner, P., unpublished data).

In the liquid crystalline phase above the azeotropic point (inverted hexagonal H_{II} phase according to Ref. 9) the mixing of the two lipids is closer to random, thus indicating dissociation of the compounds during the melting transition. The difference between 'liquid' and 'solid' non-ideal interaction energies determined through phase diagram simulations using UNIQUAC is about 1.2 kT. This difference would contribute an additional term (the 'mixing' enthalpy) to the overall transition enthalpy of approx. 0.7 kcal/mol. This prediction is in very good agreement with the experimentally observed enthalpy of melting of the azeotropic complex (8.4 kcal/mol determined in Ref. 5 and 9.4 kcal/mol according to our data) which is by 0.7–0.8 kcal/mol higher than the weighted average of the enthalpies of the pure components (8.7 kcal/mol for DPPC and 7.24 kcal/mol for palmitic acid according to Ref. 5, and 8.7 kcal/mol and 8.6 kcal/mol, respectively, according to our measurements). A similar argument can probably account also for the high transition enthalpy of 1:2 DPPC/stearic acid mixture observed by Schullery et al. [6]. This explains also the discrepancy between experimental and calculated enthalpies noted by Mabrey and Sturtevant [5] as caused by the unrealistic assumption for ideal mixing involved in their modelling of the DPPC/palmitic acid phase diagram which actually neglects the contribution from the enthalpy of mixing.

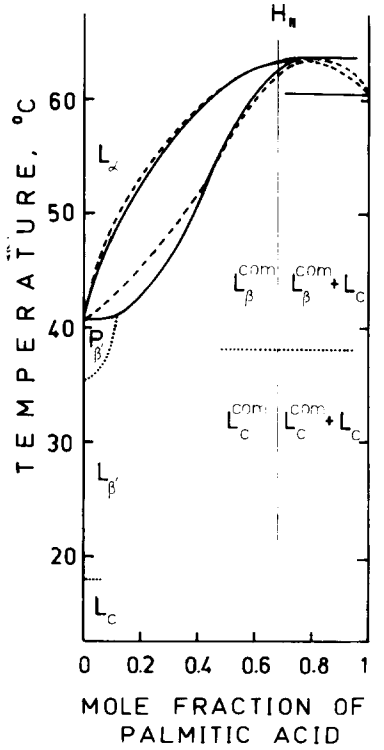

Fig. 8. Phase diagram of DPPC/palmitic acid mixture. Notation as in Fig. 6b. The pretransition is shown as a single line (second-order transition) and the region of phase separation at high fatty acid mole fractions is schematically presented. L_c^{com} denotes the compound phase.

At high fatty acid mole fractions ($\gtrsim 0.7$), the thermograms are dominated by two large transitions, one of them located approximately at the melting of the pure fatty acid and the other one at the temperature of the azeotropic point (Figs. 1–3). The former transition increases in enthalpy, while the latter one vanishes with increase of fatty acid content. In spite of the presence of a number of satellite peaks complicating this picture, it seems very likely that a separation of a more or less pure fatty acid phase from the compound phase takes place in this composition range (Fig. 8). Although solid-solid phase separations in mixtures of lipids with different head groups or acyl chains have been frequently observed (for a summary see, e.g., Ref. 17), such rather specific coexistence of a compound phase with pure component phase seems to have no analogues in the lipid mixtures. Unfortunately, this type of phase separation cannot be analysed using the criteria for single phase stability in the theory of the phase diagrams [17] since these criteria are applicable only to binary mixtures with positive E_{non} corresponding to clustering of the components, and not to 'chessboard' arrangements characterized by negative E_{non}. Therefore, at present, we are not able to determine whether the values of E^{s}_{non} calculated in the simulations of the PC/fatty acid phase diagrams really exceed some critical value and fall into the phase separation region. Qualitatively, the compound solid phase with 1 : 2 PC/fatty acid stoichiometry appears to be tight enough so that excess fatty acids cannot be incorporated into it and must form a separate phase.

With regard to the physiological effects of the fatty acids it is important to know whether domains of the compound phase remain stable also at low fatty acid contents. Since the 1 : 2 mixture melts into an inverted hexagonal phase as reported by Marsh and Seddon [9], suitably large domains of this type would give rise to non-lamellar loci in the liquid crystalline phase of the phospholipid bilayers which can be responsible for their increased permeability and fusion ability. The efficiency of this mechanism should be crucially dependent on the size of the compound phase domains at low fatty acid concentrations. They must probably comprise at least several tens of lipid molecules as to ensure the appearance of a non-lamellar locus. Although the size distribution of these domains clearly cannot be considered on basis of the present results, the PC/fatty acid phase diagrams contain a certain indication for a restricted solubility of the compound phase into the pure PC phase. As can be seen from Figs. 6–8, the experimental solidus lines (especially their horizontal parts) are well below the theoretical ones. Similarly poor fit quality is typical also for other lipid binaries with saturated PC as the low-melting component [17]. It is currently interpreted as indicative of a restricted miscibility or phase separation in the solid state. By analogy, it can be expected that sufficiently large domains of the compound phase might exist also at low concentrations of fatty acid.

The discrepancy between the results in Refs. 6 and 8 and our data about the region of intersection of the PC pretransition with the horizontal solidus line has already been noted in Results. An additional comment in this respect is in order. The considerations of Schullery et al. [6] and Kohn and Schullery [8], and also the presentation of the pretransition in Figs. 6 and 7 are based on the assumption that the pretransition is a first-order phase transition and therefore the region between its onset and completion is a region of coexistence of the $P_{\beta'}$ and $L_{\beta'}$ phases. An alternative to this is that the pretransition is not a first-order but rather a second-order process (see also the appendix to Ref. 29 for a similar assumption). In that case the phase coexistence region implied by the finite width of the pretransition should be replaced by a single line separating the $P_{\beta'}$ and $L_{\beta'}$ phases as shown in Fig. 8. The intersection of this line with the solidus results in a bicritical point [10]. This interpretation avoids the difficulties arising in connection with the Gibbs phase rule [6,8] even if the horizontal portion of the solidus is extended beyond the intersection point.

The DPPC/palmitic acid phase diagram depicted in Fig. 8 is incomplete in several respects. The regions of the L_{α}-H_{II}-micellar phase transformations obviously taking place at high temperatures with increase of fatty acid content are indeterminate. Besides, the interrelations between the various solid-solid transformations are not clear. Some of these problems will be considered in a subsequent X-ray study.

Acknowledgements

B.G.T. is grateful to Dr. J. Brankov for useful discussions on the statistical properties of mixed phases. The authors acknowledge partial financial support from the Bulgarian State Committee for Science.

References

1 Kantor, H.L. and Prestegard, J.H. (1978) Biochemistry 17, 3592–3597
2 Orly, J. and Schramm, M. (1975) Proc. Natl. Acad. Sci. USA 72, 3433–3437
3 Andreasen, T.J. and McNamee, M.G. (1980) Biochemistry 19, 4719–4726
4 Wojtczak, L. (1976) J. Bioenerg. Biomembranes 8, 293–311
5 Mabrey, S. and Sturtevant, J. (1977) Biochim. Biophys. Acta 486, 444–450
6 Schullery, S.E., Seder, T.A., Weinstein, D.A. and Bryant, D.A. (1981) Biochemistry 20, 6818–6824
7 Pauls, K.P., MacKay, A.L. and Bloom, M. (1983) Biochemistry 22, 6101–6109
8 Kohn, A.B. and Schullery, S.E. (1985) Chem. Phys. Lipids 37, 143–153
9 Marsh, D. and Seddon, J.M. (1982) Biochim. Biophys. Acta 690, 117–123
10 Landau, L.D. and Lifshitz, E.M. (1976) Statisticheskaya fizika (in Russian), 3rd Edn., Nauka, Moscow
11 Van Dijck, P.W.M., Kaper, A.J., Oonk, H.A.J. and De Gier, J. (1977) Biochim. Biophys. Acta 470, 58–66
12 Wu, S.H. and McConnell, H.M. (1975) Biochemistry 14, 847–854
13 Lee, A.G. (1977) Biochim. Biophys. Acta 472, 285–344
14 Von Dreele, P.H. (1978) Biochemistry 17, 3939–3948
15 Priest, R.G. (1980) Mol. Cryst. Liquid Cryst. 60, 167–184
16 Sugar, I.P. and Monticelli, G. (1985) Biophys. J. 48, 283–288
17 Tenchov, B.G. (1985) Prog. Surface Sci. 20, 273–340
18 Boyanov, A.I., Koynova, R.D. and Tenchov, B.G. (1986) Chem. Phys. Lipids 39, 155–163
19 Chen, S.C., Sturtevant, J.M. and Gaffney, B.J. (1980) Proc. Natl. Acad. Sci. USA 77, 5060–5063
20 Finegold, L. and Singer, M.A. (1986) Biochim. Biophys. Acta 855, 417–420
21 Hill, T.L. (1960) An Introduction to Statistical Thermodynamics, Addison-Wesley, Reading, MA
22 Huang, K. (1963) Statistical Mechanics, John Wiley, New York
23 Mendelsohn, R. and Koch, C.C. (1980) Biochim. Biophys. Acta 598, 260–271
24 Davis, P.J. and Keough, K.M.W. (1984) Chem. Phys. Lipids 35, 299–311
25 Tenchov, B.G., Brankov, J.G. and Koynova, R.D. (1984) Stud. Biophys. 103, 89–96
26 Scott, H. and Cheng, W.H., (1979) Biophys. J. 28, 117–132
27 Jacobs, R.E., Hudson, B.S. and Andersen, H.C. (1977) Biochemistry 16, 4349–4359
28 Abrams, D.S. and Prausnitz, J.M. (1975) Am. Inst. Chem. Eng. J. 21, 116–128
29 Luna, E.J. and McConnell, H.M. (1977) Biochim. Biophys. Acta 470, 303–316